



# 3D transesophageal echocardiography and radiography of mitral valve prostheses and repairs

Nadia Jafar MD<sup>1</sup> | Michael J. Moses MD<sup>1</sup>  | Ricardo J. Benenstien MD<sup>1</sup> |  
 Alan F. Vainrib MD<sup>1</sup>  | James N. Slater MD<sup>1</sup> | Henry A. Tran MD<sup>1</sup> |  
 Robert Donnino MD<sup>2,3</sup> | Mathew R. Williams MD<sup>1,4</sup> | Muhamed Saric MD, PhD<sup>1</sup>

<sup>1</sup>Leon H. Charney Division of Cardiology, New York University Langone Medical Center, New York, NY, USA

<sup>2</sup>Veterans Affairs New York Harbor Healthcare System, New York, NY, USA

<sup>3</sup>Department of Radiology, New York University School of Medicine, New York, NY, USA

<sup>4</sup>Department of Cardiothoracic Surgery, New York University School of Medicine, New York, NY, USA

## Correspondence

Muhamed Saric, Director of the Echocardiography Lab, Associate Professor of Medicine, Noninvasive Cardiology, New York University, New York, NY, USA.  
 Email: muhamed.saric@nyumc.org

This paper provides a comprehensive overview of 3D transesophageal echocardiography still images and movies of mechanical mitral valves, mitral bioprostheses, and mitral valve repairs. Alongside these visual descriptions, the historical overview of surgical and percutaneous mitral valve intervention is described with the special emphasis on the incremental value of 3D transesophageal echocardiography (3DTEE). For each mitral valve intervention, 2D echocardiography, chest x-ray, and fluoroscopy images corresponding to 3DTEE are given. In addition, key references on echocardiographic imaging of individual valves and procedures are enumerated in accompanying figures and tables.

## KEYWORDS

3D transesophageal echocardiography, imaging, mitral valve bioprostheses, mitral valve mechanical prostheses, mitral valve repair

## 1 | HISTORICAL OVERVIEW

The creation of the first successful heart–lung machine in the 1950s revolutionized the field of cardiac surgery, allowing orthotopic replacement of diseased heart valves.<sup>1</sup> Thereafter, the field rapidly progressed from the advent of mechanical and bioprosthetic valves to surgical mitral valve repair ultimately leading to modern techniques of percutaneous mitral valve repair. The collaboration of surgeons and engineers made these advancements possible and is reflected in the naming convention of many prosthetic valves (as in Starr–Edwards and Björk–Shiley valve where the former name refers to the cardiac surgeon and the latter refers to the engineer). Historical time line is outlined in Table 1.

## 2 | 3DTEE IMAGING OF NATIVE AND PROSTHETIC MITRAL VALVES

The field of 3D echocardiography was revolutionized in the past decade with the introduction of novel matrix array transducers. The standard two-dimensional transesophageal echocardiography probe typically has 64 imaging elements, whereas the three-dimensional

transesophageal echocardiography (3DTEE) probe has 3000 imaging elements. With this new probe technology, real time 3D echocardiographic imaging became feasible for the first time. Key references on echocardiographic imaging of individual valves and procedures are provided in Table 2.

Real time 3DTEE is capable of producing exceptional views of the mitral leaflets, annulus, and subvalvular structures including the novel en face views of the mitral valve from both the atrial and ventricular perspectives.<sup>2</sup> This quality allows 3DTEE to be used to diagnose mitral valve pathology, guide surgical intervention, and identify potential complications, such as paravalvular or para-annular leaks, with unprecedented clarity.<sup>3</sup>

Native mitral valves, mitral bioprostheses, and repair can easily be visualized from both left atrial and left ventricular perspectives. Imaging of mechanical mitral prostheses is best accomplished from the left atrial perspective as left ventricular aspects of mechanical prostheses are often obscured by reverberation and shadowing artifacts.

3DTEE images of the mitral valve in this manuscript are displayed primarily from the left atrial perspective in the so-called “surgical” view. In this view, the mitral valve is in the center of the image resembling a clock face; the aortic valve is seen at 12 o'clock, the left atrial appendage at 9 o'clock, and the interatrial

**TABLE 1** Historical development of major prosthetic valves and repairs

Year <sup>a</sup>	Category	Valve or repair type
1960	Mechanical valve	Starr–Edwards ball-in-cage
1969	Mechanical valve	Björk–Shiley single-tilting disk
1971	Valve repair	Annuloplasty ring
1975	Bioprosthetic valve	Carpentier–Edwards porcine
1977	Mechanical valve	Medtronic–Hall single-tilting disk
1977	Mechanical valve	St. Jude Medical bi-leaflet-tilting disk
1978	Mechanical valve	Omniscience single-tilting disk
1983	Valve repair	“French correction”
1984	Bioprosthetic valve	Carpentier–Edwards pericardial
1986	Mechanical valve	CarboMedics bi-leaflet-tilting disk
1995	Valve repair	Partial annuloplasty ring
2001	Valve repair	Edge-to-edge repair (Alfieri stitch)
2013	Valve repair	MitraClip
2000s	Valve-in-valve	TAVR valves within failed mitral bioprostheses

<sup>a</sup>Refers to year when first commercially available in the United States.

septum at 3 o'clock. It is important to emphasize that this view differs from the true anatomic view of the mitral valve, as depicted in Figure 1.

### 3 | RADIOGRAPHY AND FLUOROSCOPY OF PROSTHETIC VALVES

Radiographic imaging (such as chest x-ray and chest computed tomography) plays an important role in evaluating the appearance of prosthetic valves and complements the information obtained by echocardiography. The radiopaque nature of the occluders, sewing rings, and other components of prosthetic valves and valve repairs allows for visualization with relative clarity and ease. Typically, based on the radiographic appearance, one can deduce the type and location of a prosthetic valve or valve repair. In addition to its general clinical utility, such information is of particular value in the emerging field of percutaneous valve-in-valve procedures.

Fluoroscopy is an easy and readily available technique that remains the preferred modality to visualize the mobility of mechanical prosthetic valve occluders in real time. It also allows for measurement of the opening and closing angles of the mechanical prosthetic valve

**TABLE 2** Key references on echocardiographic imaging of valve prostheses and repairs

Prosthesis/repair	Article
Starr–Edwards mechanical prosthesis	Alton ME, Pasierski TJ, Orsinelli DA, Eaton GM, Pearson AC. Comparison of transthoracic and transesophageal echocardiography in evaluation of 47 Starr–Edwards prosthetic valves. <i>J Am Coll Cardiol.</i> 1992;20:1503–1511.
Björk–Shiley mechanical prosthesis	Taams MA, Gussenhoven EJ, Cahalan MK, Roelandt JR, van Herwerden LA, The HK, Bom N, de John N. Transesophageal Doppler color flow imaging in the detection of native and Björk–Shiley mitral valve regurgitation. <i>J Am Coll Cardiol.</i> 1989;13:95–99.
Medtronic–Hall mechanical prosthesis	Bernstein O, Haddy S. Three-dimensional echocardiography of a Medtronic Hall-type tilting disk valve. <i>Echocardiography.</i> 2012;29:E129–130.
St. Jude Medical mechanical prosthesis	Lange HW, Olson JD, Pedersen WR, Kane MA, Daniel JA, Mooney MR, Goldenberg IF. Transesophageal color Doppler echocardiography of the normal St. Jude Medical mitral valve prosthesis. <i>Am Heart J.</i> 1991;122:489–494. Stoddard MF, Dawkins PR, Longaker RA. Mobile strands are frequently attached to the St. Jude Medical mitral valve prosthesis as assessed by two-dimensional transesophageal echocardiography. <i>Am Heart J.</i> 1992;124:671–674.
Omniscience mechanical prosthesis	Mikhail A. A hemodynamic comparison of Omniscience and Medtronic Hall aortic prostheses. <i>J Heart Valve Dis.</i> 1996; 5:675–677.
CarboMedics mechanical prosthesis	Chambers J, Cross J, Deverall P, Sowton E. Echocardiographic description of the CarboMedics bileaflet prosthetic heart valve. <i>J Am Coll Cardiol.</i> 1993;21:398–405.
Bioprosthetic valves	Alam M, Serwin JB, Rosman HS, Polanco GA, Sun I, Silverman NA. Transesophageal echocardiographic features of normal and dysfunctioning bioprosthetic valves. <i>Am Heart J.</i> 1991;121(4 Pt 1):1149–1155. Daniel WG, Mugge A, Grote J, Hausmann D, Nikutta P, Laas J, Lichtlen PR, Martin RP. Comparison of transthoracic and transesophageal echocardiography for detection of abnormalities of prosthetic and bioprosthetic valves in the mitral and aortic positions. <i>Am J Cardiol.</i> 1993;71:210–215.
Annuloplasty	Kronzon I, Sugeng L, Perk G, Hirsh D, Weinert L, Garcia Fernandez MA, Lang RM. Real-time 3-dimensional transesophageal echocardiography in the evaluation of post-operative mitral annuloplasty ring and prosthetic valve dehiscence. <i>J Am Coll Cardiol.</i> 2009;53:1543–1547. Maslow A, Mahmood F, Poppas A, Singh A. Three-dimensional echocardiographic assessment of the repaired mitral valve. <i>J Cardiothorac Vasc Anesth.</i> 2014;28:11–17.
Nonresectional valve repair	Faletra FF, Pedrazzini G, Pasotti E, Petrova I, Drasutiene A, Dequarti MC, Muzzarelli S, Moccetti T. Role of real-time three dimensional transesophageal echocardiography as guidance imaging modality during catheter based edge-to-edge mitral valve repair. <i>Heart.</i> 2013;99:1204–1215. Rankin JS, Gaca JG, Brunsting LA 3rd, Daneshmand MA, Milano CA, Glower DD, Smith PK. Increasing mitral valve repair rates with nonresectional techniques. <i>Innovations (Phila).</i> 2011;6:209–220.

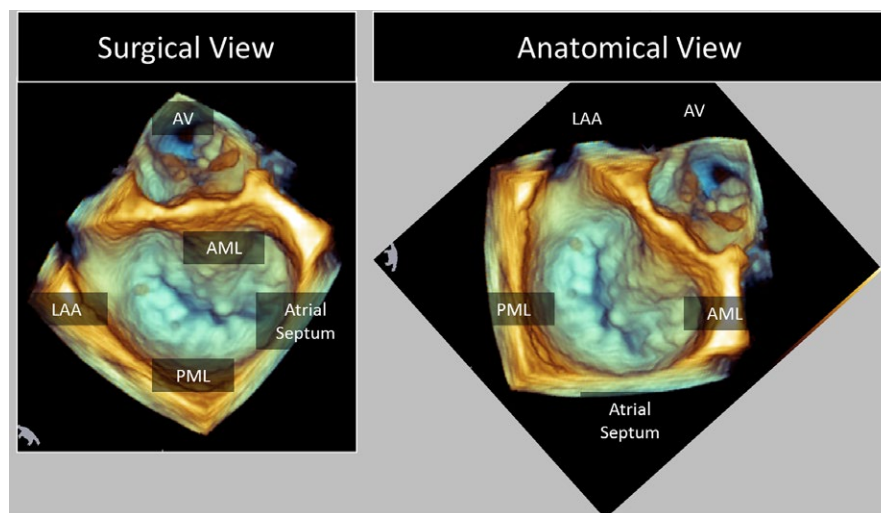


**FIGURE 1** Surgical vs anatomic view of mitral valve. The left atrial perspective of the native mitral valve in the surgical view (A) vs the true anatomic view (B)

leaflets which are defined as the distance between the two leaflets in the fully open and closed position, respectively. Assessment of these angles provides a means to establish the normality of prosthesis function; deviations from normal angle values may indicate obstructions or mechanical failure. We provide the numeric values for opening and closing angles in this manuscript for single-leaflet and bi-leaflet mechanical prostheses in Table 3.

An algorithm for imaging of mitral prosthetic valves and repairs is provided in Figure 2.

## 4 | MECHANICAL VALVES

### 4.1 | Starr-Edwards ball-in-cage mechanical prosthesis

In the fall of 1957, Dr. Albert Starr was a young cardiac surgeon at the University of Oregon Medical School when he met Miles Lowell Edwards, a retired engineer. Their work led to the development of a ball-in-cage mechanical prosthesis, based on the design of an 1858 bottle stopper.<sup>1</sup> This valve was implanted in the first human patient in August 1960.<sup>4</sup>

After various design adjustments, the 6120 mitral valve model was established in 1965.<sup>5</sup> This mitral model consists of a four-strut cobalt-chromium stellite alloy cage and a barium-impregnated silastic ball. In contrast, the aortic valve version has three struts.<sup>6</sup>

Flow through the Starr-Edwards valve first converges as it passes through the sewing ring and then deviates in a circumferential manner as it passes around the periphery of the ball-shaped occluder. The Starr-Edwards valve has a smaller effective orifice area and higher transvalvular gradients as compared to more modern mechanical prostheses due to relatively inefficient flow around the ball.<sup>7</sup> Retrograde flow in early systole is necessary for normal valve closure with a characteristic color Doppler pattern.<sup>8</sup>

The Starr-Edwards valve has a relatively high thrombogenic potential, which requires vigilant and aggressive anticoagulation.<sup>9</sup> Despite these problems, the Starr-Edwards mechanical valve remains on the

market and continues to be implanted as a cost-effective option for surgical valve replacement.<sup>10</sup>

The Starr-Edwards valve is depicted in Figure 3 and Movies S1A,B.

### 4.2 | Björk-Shiley tilting disk mechanical prosthesis

Following the development of the Starr-Edwards valve, multiple single-tilting disk valves were introduced. One of the first commercially successful tilting disk valves was the Björk-Shiley valve, invented by the Swedish cardiac surgeon Viking Björk and the American engineer Donald Shiley.<sup>11,12</sup>

Introduced in 1969, the Björk-Shiley mechanical prosthetic valve is composed of a single-tilting disk that is held in place by an inlet strut and an outlet strut.<sup>6</sup> The Björk-Shiley has been revised several times from its initial design to reduce thrombogenicity and improve hemodynamics. Typically, the disk is 1 mm thick with a graphite core surrounded by low-temperature isotropic carbon or pyrolytic carbon.<sup>13</sup> The opening angle of the tilting disk ranges from 60 to 70° in different models with a closing angle of 0°. The backflow of two holosystolic jets through a small space between the disk and housing is necessary for normal disk closure.<sup>14</sup>

In 1986, after several hundred valves with a so-called convexo-concave design fractured resulting in disk embolization, the Food and Drug Administration (FDA) recalled the Björk-Shiley valve.<sup>15</sup> Although the valve is no longer implanted, one should be familiar with its appearance and function as patients with this prosthesis may still be encountered in clinical practice.

The Björk-Shiley valve is depicted in Figure 4 and Movies S2A,B.

### 4.3 | Medtronic-Hall single-tilting disk prosthesis

Norwegian cardiac surgeon Karl Victor Hall worked with the engineer Robert Kaster to design a single-tilting disk valve that served as the blueprint for the Medtronic-Hall prosthesis.<sup>6</sup> This mechanical prosthesis is composed of a Teflon sewing ring that surrounds radiopaque titanium housing and a radiolucent carbon-coated disk. The disk is

**TABLE 3** Normal values for mechanical mitral prosthetic valves

Valve type	Opening angle degrees	Closing angle degrees	Valve size mm	Peak gradient mm Hg	Mean gradient mm Hg	Peak velocity m/s	Pressure Half-time ms	Effective orifice area cm <sup>2</sup>
Starr-Edwards caged ball	Not applicable	Not applicable	26		10			1.4
			28		7 ± 2.75			1.9 ± 0.57
			30	12.2 ± 4.6	6.99 ± 2.5	1.7 ± 0.3	125 ± 25	1.65 ± 0.4
			32	11.5 ± 4.2	5.08 ± 2.5	1.7 ± 0.3	110 ± 25	1.98 ± 0.4
			34		5			2.6
Bjork-Shiley tilting disk	60–70	0	23			1.7	115	
			25	12 ± 4	6 ± 2	1.75 ± 0.38	99 ± 27	1.72 ± 0.6
			27	10 ± 4	5 ± 2	1.6 ± 0.49	89 ± 28	1.81 ± 0.54
			29	7.83 ± 2.93	2.83 ± 1.27	1.37 ± 0.25	79 ± 17	2.1 ± 0.43
			31	6 ± 3	2 ± 1.9	1.41 ± 0.26	70 ± 14	2.2 ± 0.3
			27			1.4	78	
Medtronic-Hall tilting disk	70	0	29			1.57 ± 0.1	69 ± 15	
			31			1.45 ± 0.12	77 ± 17	
			23		4	1.5	160	1
St. Jude Medical bi-leaflet	85	25–30	25		2.5 ± 1	1.34 ± 1.12	75 ± 4	1.35 ± 0.17
			27	11 ± 4	5 ± 1.82	1.61 ± 0.29	75 ± 10	1.67 ± 0.17
			29	10 ± 3	4.15 ± 1.8	1.57 ± 0.29	85 ± 10	1.75 ± 0.24
			31	12 ± 6	4.46 ± 2.22	1.59 ± 0.33	74 ± 13	2.03 ± 0.32
			23			1.9 ± 0.1	126 ± 7	
CarboMedics bi-leaflet	78	25	25	10.3 ± 2.3	3.6 ± 0.6	1.3 ± 0.1	93 ± 8	2.9 ± 0.8
			27	8.79 ± 3.46	3.46 ± 1.03	1.61 ± 0.3	89 ± 20	2.9 ± 0.75
			29	8.78 ± 2.9	3.39 ± 0.97	1.52 ± 0.3	88 ± 17	2.3 ± 0.4
			31	8.87 ± 2.34	3.32 ± 0.87	1.61 ± 0.29	92 ± 24	2.8 ± 1.14
			33	8.8 ± 2.2	4.8 ± 2.5	1.5 ± 0.2	93 ± 12	

### Imaging Algorithm for Mitral Prosthetic Valves

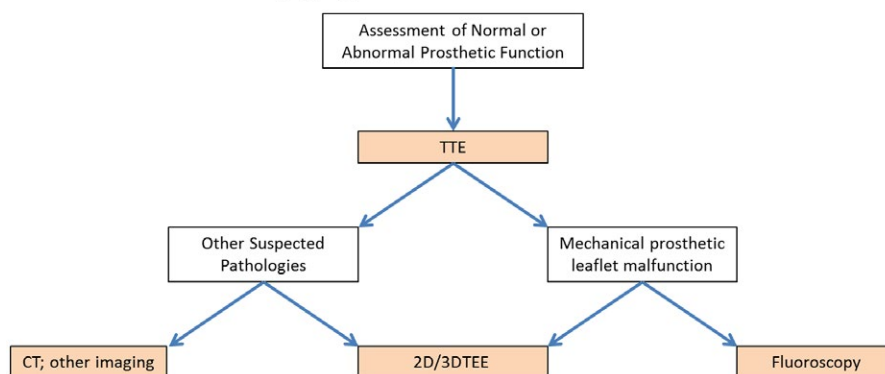
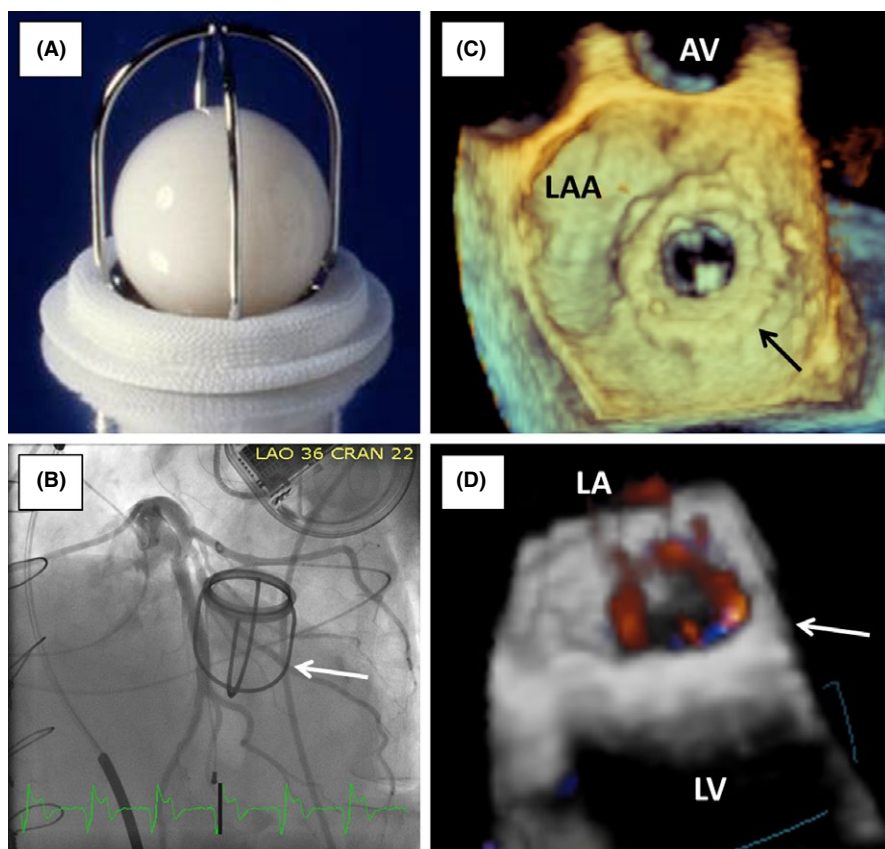


**FIGURE 2** Imaging algorithm for mitral prosthetic valves. CT = computed tomography; TEE = transesophageal echocardiogram; TTE = transthoracic echocardiogram

**FIGURE 3** Starr-Edwards mechanical valve. A. Photograph of Starr-Edwards mitral valve prosthesis. Reprinted by permission from Edwards LifeSciences. B. Radiologic appearance of Starr-Edwards mitral valve (arrow) during cardiac catheterization in a cranially tilted left anterior oblique view. Movie S1A corresponds to this panel. C. 3DTEE appearance of Starr-Edwards valve (arrow) from the left atrial perspective in the standard surgical view. AV = aortic valve; LAA = left atrial appendage. Movie S1B Corresponds to this panel and adds the LV perspective as well. D. 3DTEE color Doppler image of Starr-Edwards valve (arrow) demonstrates the characteristic appearance of normal regurgitant jets ("backflow jets")



mounted on a sigmoid strut and lifts out of the housing, rotating once opened with an opening angle of  $70^\circ$  and a closing angle of  $0^\circ$ .<sup>16</sup>

After the valve opens, two antegrade jets pass through a major orifice and a minor orifice, with the flow through the major orifice having a slightly higher velocity than the flow through the minor orifice.<sup>17</sup> The relative size of the minor orifice of the Medtronic-Hall prosthesis is greater when compared to earlier tilting disk valves. This larger minor orifice, along with the disk design, enhances washing of the valve and eliminates regions of low-velocity flow.<sup>18</sup>

During valve closure, gaps between the disk and the housing create regurgitant jets. The central orifice releases a characteristic central regurgitant jet around the strut. Smaller peripheral regurgitant jets may occur around the rim of the disk, although regurgitation may not occur

around the entire circumference.<sup>10</sup> Overall, this mechanical prosthesis is characterized by low thrombogenicity, excellent hemodynamics, and durability.<sup>19</sup> The Medtronic-Hall mechanical valve is depicted in Figure 5 and corresponding movies.

#### 4.4 | St. Jude Medical bi-leaflet mechanical prosthesis

The notion of unimpeded central flow within mechanical prostheses was pioneered with the development of the St. Jude bi-leaflet mechanical valve in 1977. The St. Jude valve was the result of the collaboration between Xinon C. Posis, an engineer, Demetre Nicoloff, an American cardiovascular surgeon, and Manny Villafana, the founder



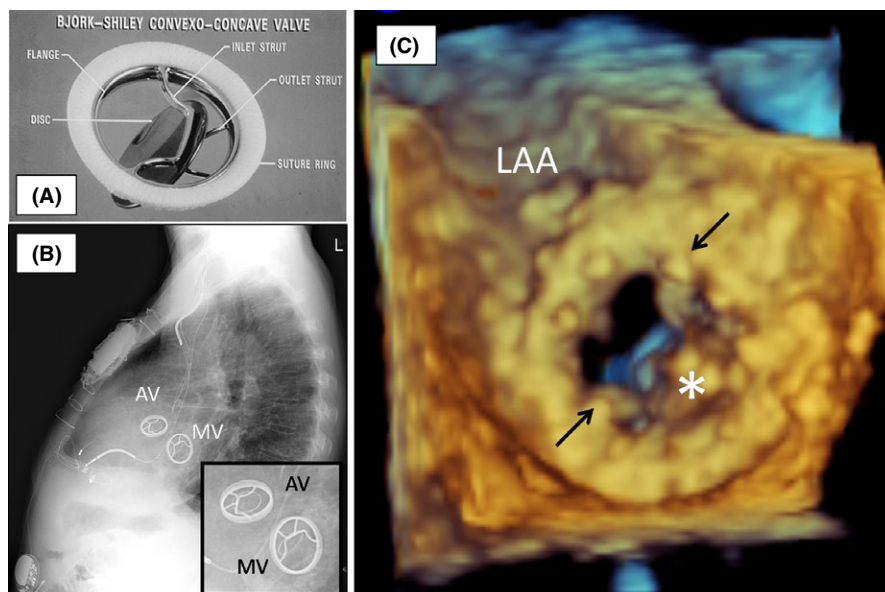


**FIGURE 4** Björk–Shiley mechanical valve. A. Photograph of Björk–Shiley mitral valve prosthesis. Reprinted by permission from Pfizer. B. Chest x-ray of Björk–Shiley mitral valve (MV) and aortic valve (AV) in lateral view. Movie S2A demonstrates the radiologic appearance of a mitral Björk–Shiley valve in another patient during cardiac catheterization. C. 3DTEE appearance of Björk–Shiley valve from the left atrial perspective in the standard surgical view. Arrows point to the struts of the prosthetic valve and the asterisk to the occluder disk. LAA = left atrial appendage. Movie S2B corresponds to this panel

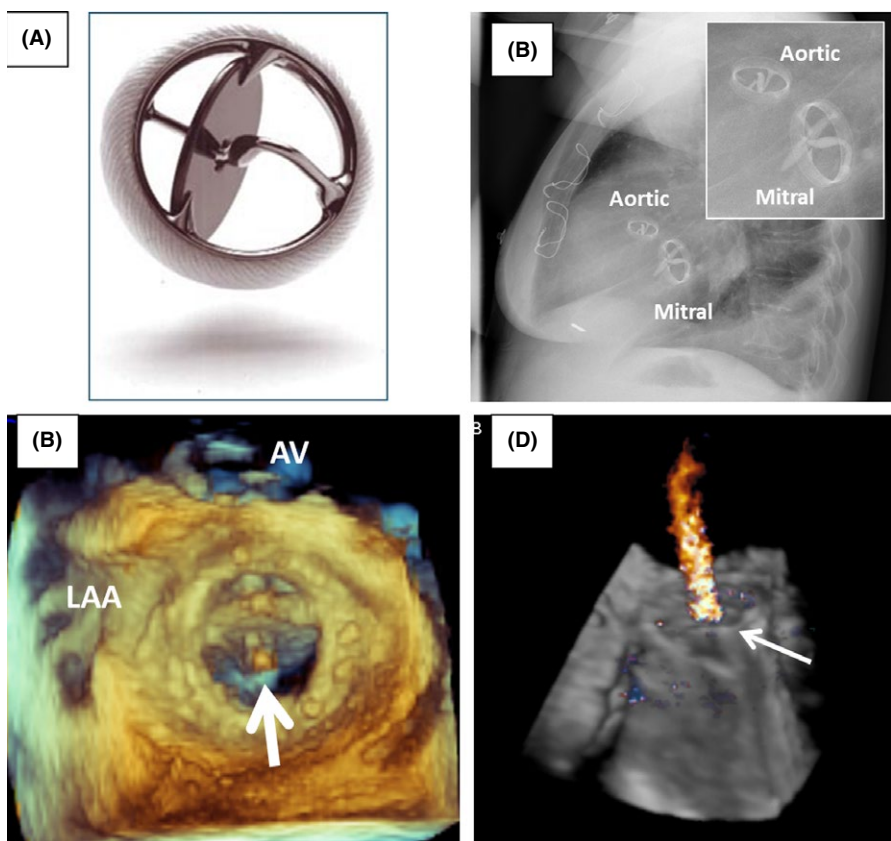


**FIGURE 5** Medtronic–Hall mechanical valve. A. Photograph of Medtronic–Hall mitral valve prosthesis. Reprinted with permission from Medtronic. B. 3DTEE appearance of Medtronic–Hall valve in the standard surgical view from the left atrial perspective. Movie S3A corresponds to this panel. C. Radiologic appearance of the Medtronic–Hall valve in the mitral position (larger of the two prosthetic valves) and in the aortic position (smaller of the two prosthetic valves). Movie S3B corresponds to this panel and demonstrates the radiologic appearance of the two prosthetic valves during cardiac catheterization. D. Color Doppler 3DTEE image of the mitral Medtronic–Hall valve (arrow) demonstrates the characteristic central jet of mitral regurgitation in the left atrium which is physiologic

of Cardiac Pacemakers, Inc.<sup>3</sup> As its introduction, this valve has seen few modifications and is currently the most commonly implanted mechanical prosthesis.<sup>19</sup>

The bi-leaflet-tilting disk design consists of two semicircular leaflets made of pyrolytic carbon impregnated with tungsten to improve radiopacity. Two pivot housings also composed of pyrolytic carbon, are located on the inflow side of the prosthesis (this refers to the left atrial side when the prosthesis is implanted in the mitral position). The

semicircular disks have an opening angle of 85° and a closing angle of 25–30°.

After the valve opens, three orifices are produced allowing for more central and less turbulent antegrade flow as compared to the ball-in-cage or single-tilting disk mechanical prostheses.<sup>20</sup> The central orifice of this valve is significantly smaller than the two lateral ones.

During valve closure, a complicated array of regurgitant jets arises causing different jet patterns to be seen based on imaging plane

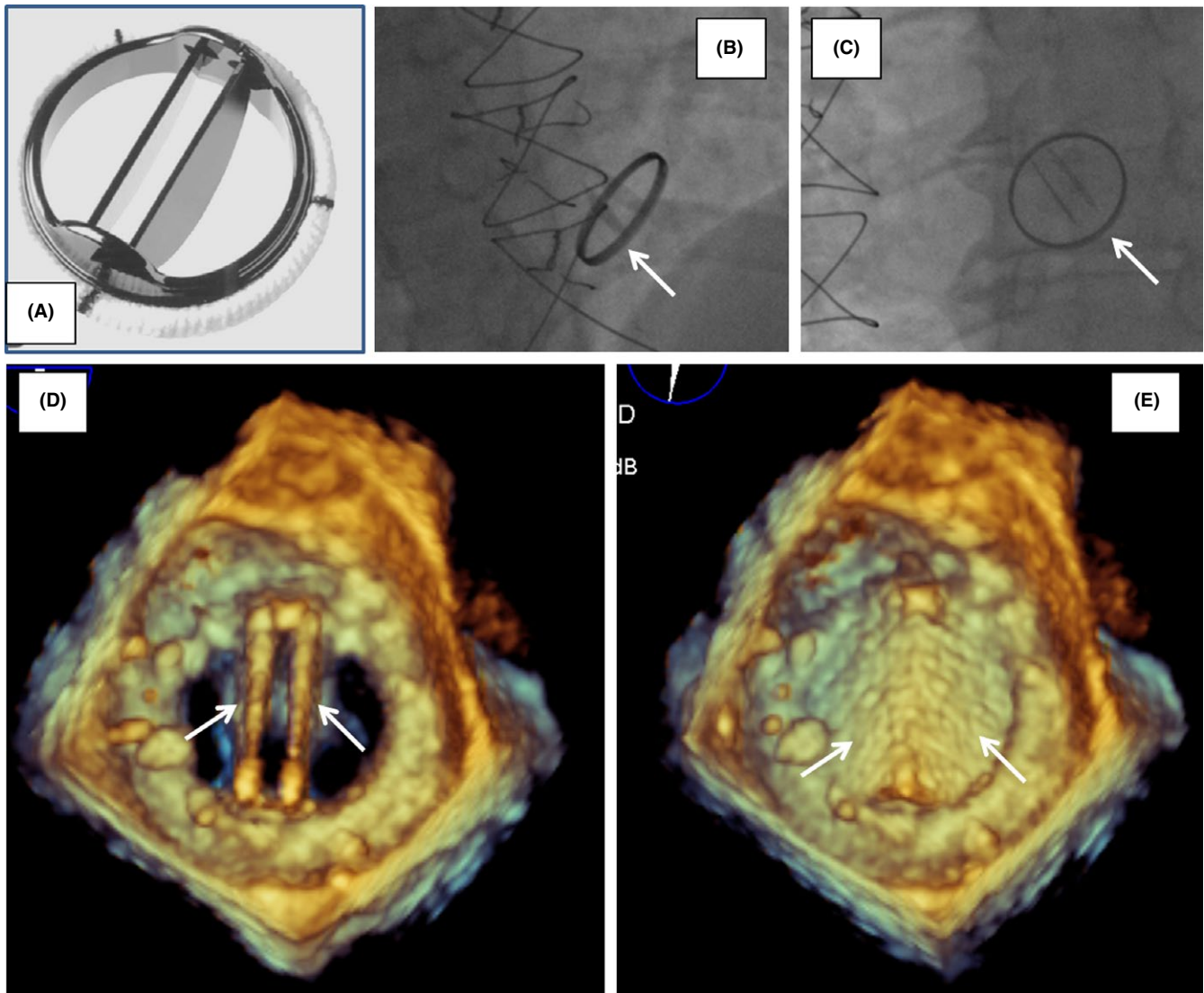


**FIGURE 6** St. Jude mechanical mitral valve. A. Photograph of St. Jude mitral valve prosthesis. Reprinted by permission from St. Jude Medical. B and C. Radiologic appearance of St. Jude mitral valve (arrow) at cardiac catheterization during diastole. Movie S4A corresponds to this panel. D and E. 3DTEE appearance of St. Jude valve in the open (D) and closed position (E) in the standard surgical view from the left atrial perspective. White arrows point to prosthetic leaflets in both panels. Movie S4B corresponds to this panel

orientation. In the plane parallel to the leaflet axes, regurgitant jets arising from the valve periphery converge toward the center of the valve in the shape of an inverted V. In the plane orthogonal to the leaflet axes, however, regurgitant jets diverge from the central axis toward the periphery of the valve to form an upright V. A small regurgitant jet from the central orifice accompanies these peripheral jets in all planes.<sup>10</sup> In general, the St. Jude mechanical prosthesis has excellent hemodynamics and a low rate of valve-related mortality.<sup>21</sup> The St. Jude valve is depicted in Figure 6 and Movies S4A,B.

#### 4.5 | Omniscience single-leaflet mechanical prosthesis

The Omniscience single-tilting disk prosthesis, an improved version of the Lillehei-Kaster disk valve, became available in 1978.<sup>8</sup> This valve

contains a pyrolytic carbon disk that is housed in a titanium cage, surrounded by a polytetrafluoroethylene sewing ring. The curvilinear disk pivots to a maximum opening angle of 80° and a closing angle of 12°.<sup>6</sup>

After the valve opens, the low-profile design enables central antegrade flow. The gradient across the prosthesis, however, is somewhat elevated compared to those of the other mechanical disk valves. This gradient can be further elevated if the disk does not open properly. Decreased opening angles have been reported in multiple studies, reducing hemodynamic performance and predisposing to thrombus formation. In 1982, a revised version of the Omniscience prosthesis was introduced, resulting in decreased complication rates and better clinical results.<sup>15</sup>

During valve closure, small gaps at the perimeter of the valve create minimal regurgitation which reduces transvalvular energy loss.<sup>22,23</sup> The Omniscience mechanical valve is depicted in Figure 7 and Movie S5A,B.



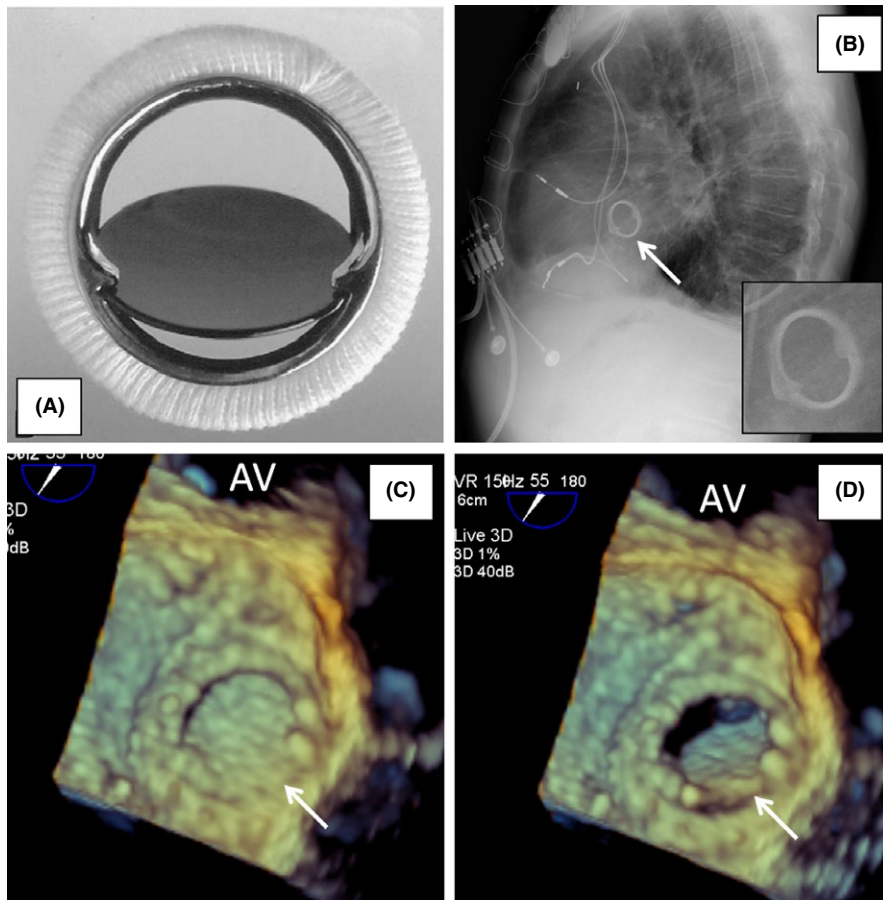


**FIGURE 7** Omniscience mechanical valve. A. Photograph of Omniscience mitral valve prosthesis. Reprinted by permission from Medical CV. B. Radiologic appearance of Omniscience mitral valve (arrow) on a lateral chest x-ray. Movie S5A corresponds to this panel. C and D. 3DTEE appearance of Omniscience valve (arrow) in the open (C) and closed position (D) from the left atrial perspective in the standard surgical view. AV = aortic valve. Movie S5B corresponds to this panel

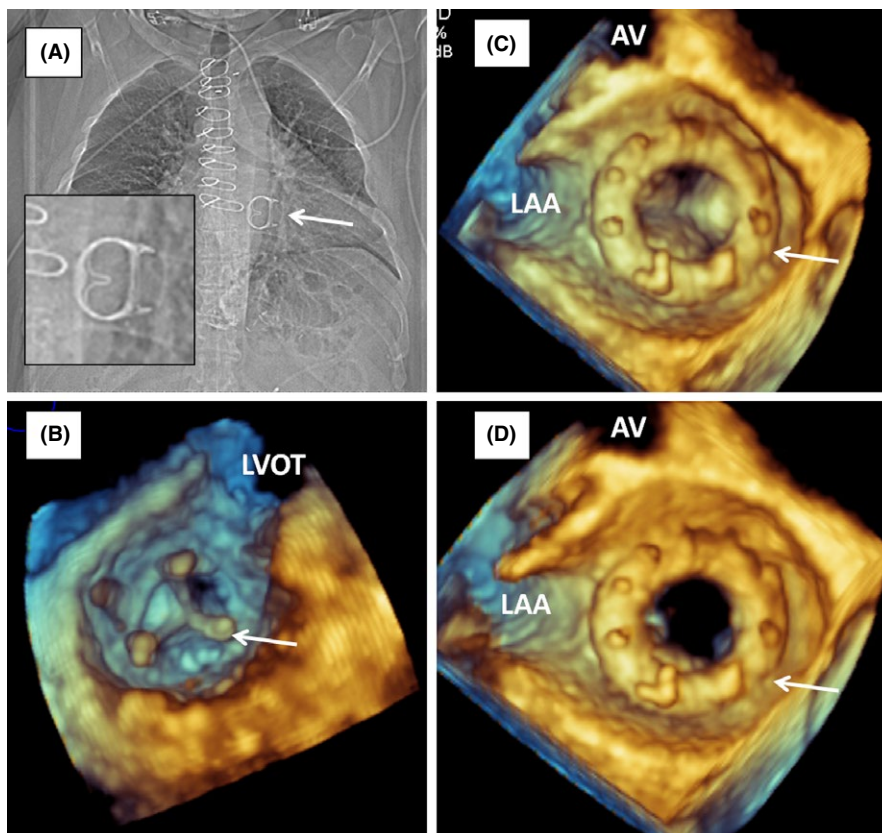


**FIGURE 8** Bioprosthesis mitral valve. A. Radiologic appearance of bioprosthesis mitral valve (arrow) in a chest x-ray. Movie S6A corresponds to this panel and demonstrates the radiologic appearance of a mitral bioprosthesis valve during cardiac catheterization. B. 3DTEE appearance of bioprosthesis mitral valve (arrow) from the left ventricular perspective. LVOT = left ventricular outflow tracts. Movie S6B corresponds to this panel. C and D. 3DTEE appearance of bioprosthesis mitral valve (arrow) from the left atrial perspective in the standard surgical view in the open (C) and closed position (D). AV = aortic valve; LAA = left atrial appendage



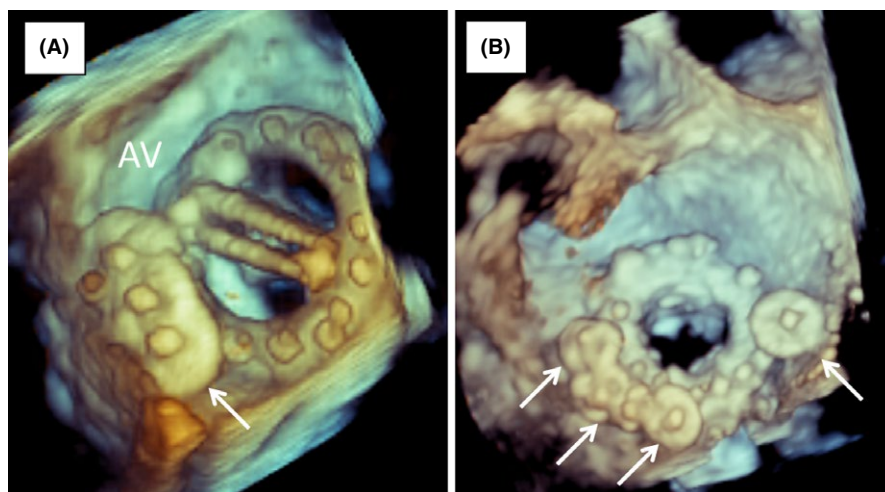


**FIGURE 9** Percutaneous repair of prosthetic paravalvular leaks (PVLs). Multiple plugs (arrow) are used to close PVLs in a patient with a mechanical St Jude mitral prosthesis (A) and in a patient with a bioprosthetic mitral valve (B)

#### 4.6 | CarboMedics

The CarboMedics bi-leaflet valve was developed by Jack Bokros and was approved for commercial use in the United States by the Food and Drug Administration in 1993.<sup>24</sup> The valve looks strikingly similar to the St. Jude Medical mechanical bi-leaflet prosthesis, apart from some important differences. The CarboMedics prosthesis is composed of two carbon-coated disks with an opening angle of 78° and a closing angle of 25°. The CarboMedics valve has a different hinge design, as compared to the St. Jude valve, and its housing can rotate within the sewing ring allowing for orientation adjustments during implantation. Furthermore, the antegrade gradient across the CarboMedics prosthesis is slightly higher than that of the St. Jude valve.<sup>5</sup>

Despite these distinctions, there is no significant difference in closing regurgitant volumes or backflow-patterns between these two prostheses in the mitral position.<sup>25</sup> The rates of survival, bleeding, thromboembolism, and prosthetic valve dysfunction at 10 years after valve implantation were similar for both the St. Jude Medical and the CarboMedics prostheses.<sup>24</sup>

### 5 | BIOPROSTHETIC MITRAL VALVES

To overcome the drawbacks of the mechanical prosthetic valve, the French cardiovascular surgeon Alain Carpentier was driven to expand the options for valvular disease through the invention of bioprosthetic valves. The most common types of bioprosthetic valves are either porcine or bovine in origin. The porcine valves are pig aortic valves while bovine valves are fashioned from pericardial tissue to resemble the native aortic valve. These original bioprostheses were all stented but more recently stentless bioprostheses have been developed.

The Carpentier–Edwards porcine valve, the prototypical bioprosthesis, has been commercially available since 1975. Carpentier pioneered the implantation of porcine aortic valve heterografts into humans after preservation and sterilization. He encased the porcine valves, fixed with glutaraldehyde, in an asymmetric elgiloy

wire stent to ease surgical implantation.<sup>3,8,26</sup> The radiopaque stent is covered with polytetrafluoroethylene cloth to augment tissue ingrowth.<sup>27,28</sup> He coined the term “bioprosthesis” to describe his invention.<sup>29</sup>

First generation bovine pericardial prostheses were plagued by early structural dysfunction, but the revised Carpentier–Edwards bovine pericardial valve has proven to be durable with excellent long-term results.<sup>30</sup> Initially implanted for clinical use in 1984, the Carpentier–Edwards bovine pericardial valve is one of the first bio-mechanically engineered valves. Created using computer-aided design systems, this bioprosthesis has superior hemodynamics to the porcine heterografts.<sup>8</sup> The valve is constructed from glutaraldehyde-fixed bovine pericardial tissue covering three flexible nickel–cobalt alloy struts, which are attached to a sewing ring.<sup>31</sup> The three struts that protrude into the left ventricular cavity are the most easily recognizable feature of the Carpentier–Edwards valve.

Transprosthetic regurgitation may occur with normally functioning bioprostheses, particularly with those made of bovine pericardium. If mild backflow does occur, it is usually in the form of a single, central jet.<sup>32,33</sup> The stentless prostheses are more likely to exhibit this transprosthetic regurgitation than stented valves.<sup>34</sup> Other manufacturers of bioprosthetic valves with characteristics similar to those of Carpentier–Edwards valves include Medtronic, St. Jude Medical, and Sorin Group.

A bioprosthetic mitral valve is depicted in Figure 8 and Movie S6A,B.

### 6 | PROSTHETIC PARAVALVULAR LEAK REPAIR

The importance of identifying paravalvular leaks utilizing 3DTEE is becoming more commonplace. These paravalvular leaks tend to be more common in mechanical valve implantation of the mitral valve, but the exact incidence is unknown and differs widely between registries.<sup>35</sup> The incidence currently cited in the literature for mitral paravalvular leaks ranges from 7% to 17% of cases.<sup>35</sup>

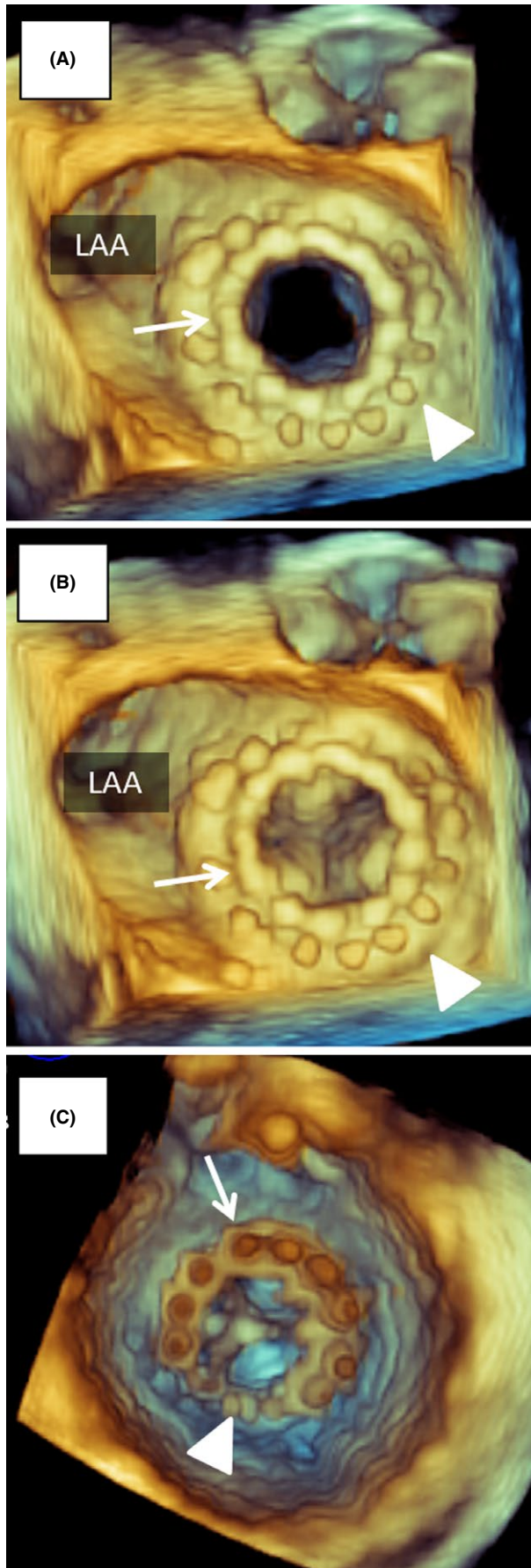


**FIGURE 10** Percutaneous mitral valve-in-valve. Percutaneously implanted Sapien valve (arrow) is seen inside a degenerated surgical mitral bioprosthesis (arrowhead). The left atrial perspective is seen in Panel A (during diastole) and in Panel B (during systole). The left ventricular perspective during systole is seen in Panel C. Movie S7 corresponds to these panels

Echocardiography is the gold-standard for the diagnosis of para-valvular leaks and 3DTEE has been shown to diagnose paravalvular leaks with greater accuracy, allowing for increased spatial visualization of the defect. This allows the provider to garner a greater degree of information regarding the leak in the perioperative period and subsequently plan the proper intervention (Figure 9).<sup>36</sup>

## 7 | PERCUTANEOUS MITRAL VALVE-IN-VALVE PROCEDURE

As bioprosthetic valves become more widely used in the management of mitral valve repair, clinicians must be aware of the potential possibility of degeneration of the bioprosthetic implant, thus necessitating a revision procedure. These revision operations are typically associated with increased morbidity and mortality for the patient, especially in elderly patient with complicated medical comorbidities.<sup>37</sup> Over the course of the past few years, transcatheter valve implantation has emerged as a viable and safe option in the treatment and replacement of degenerated bioprosthetic valves using valve-in-valve implantation (Figure 10). The transapical approach is currently favored as it is “easy to setup and offers a straight and short route to the mitral plane allowing for coaxial alignment of the transcatheter within the degenerated bioprosthesis.”<sup>37</sup> There still remains a paucity of information in the current literature regarding the technique and complications of valve-in-valve implantation for the correction of mitral valve degeneration; many of these factors will be elucidated in the future as additional patients receive these bioprosthetic valves, and further clinical outcomes studies are performed.

## 8 | MITRAL VALVE REPAIRS

Mitral valve repairs can be performed with or without an annuloplasty ring. In 1957, ringless annuloplasty for mitral valve repair was first introduced. Twelve years later, Alain Carpentier pioneered the use of an annuloplasty ring.<sup>37</sup> Today, numerous types of annuloplasty rings exist.<sup>38</sup> Based on geometry, rings can be identified as complete (D-shaped rings) or partial (C-shaped rings, also referred to as annuloplasty bands). Only occasionally are modern mitral valve repairs performed without an annuloplasty ring or band, typically through plication techniques.<sup>39–41</sup>

Another mode of ringless repair is known as the edge-to-edge technique, colloquially referred to as the Alfieri stitch.<sup>38</sup> The Alfieri technique requires suturing the anterior and posterior mitral valve leaflets, typically in the central portion of the mitral valve, creating

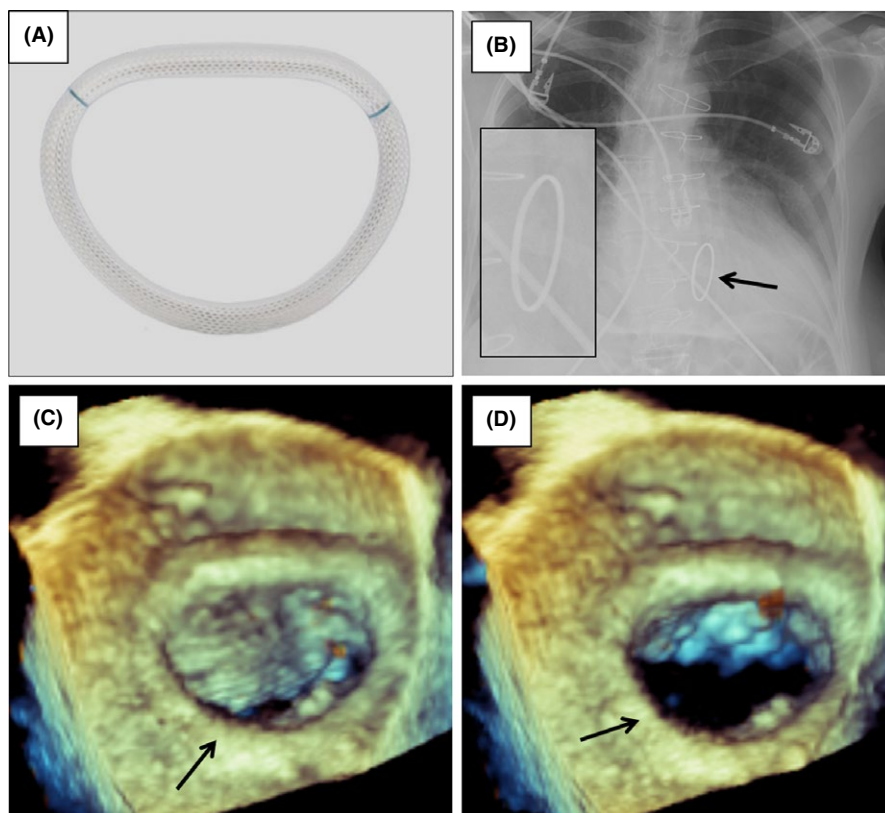


**FIGURE 11** Mitral annuloplasty ring. A. Photograph of mitral annuloplasty ring. Reprinted by permission from Edwards LifeSciences. B. Radiologic appearance of annuloplasty ring (arrow) in a chest x-ray. Movie S8A corresponds to this panel and demonstrates the radiologic appearance of an annuloplasty ring during cardiac catheterization. C and D. 3DTEE appearance of annuloplasty ring (arrow) from the left atrial perspective in the standard surgical view in the closed (C) and open position (D). Movie S8B corresponds to this panel

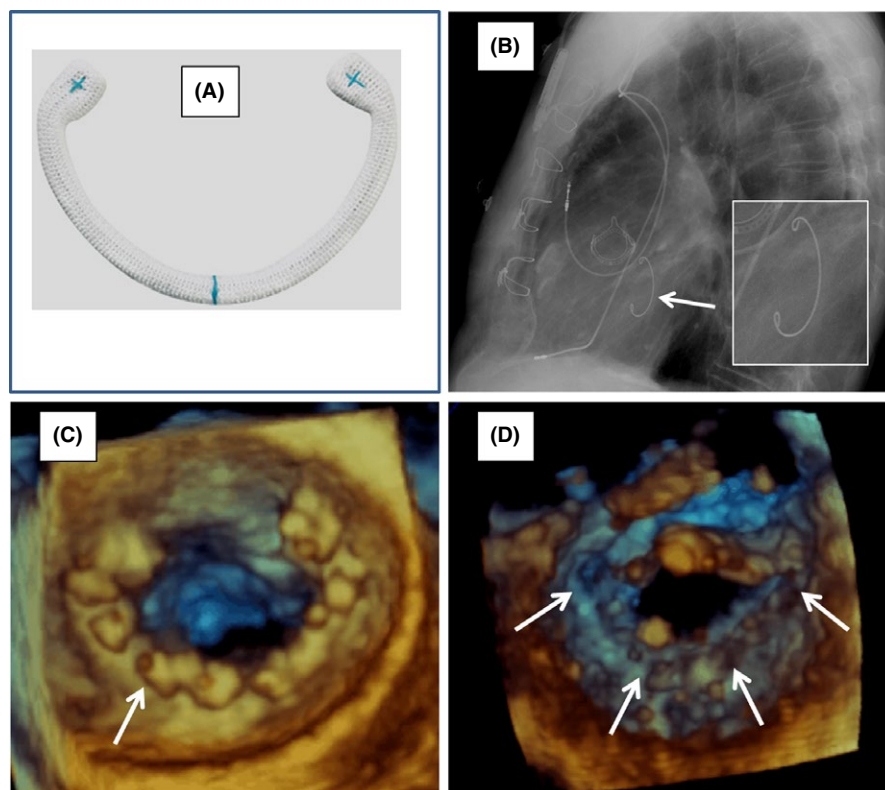


**FIGURE 12** Mitral annuloplasty band. A. Photograph of mitral annuloplasty band. Reprinted by permission from Medtronic. B. Radiologic appearance of annuloplasty band (arrow) in a lateral chest x-ray. Movie S9A corresponds to this panel and demonstrates the radiologic appearance of an annuloplasty band in another patient during cardiac catheterization. C and D. 3DTEE appearance of annuloplasty band (arrow) from the left atrial (C) and left ventricular perspective (D) in the standard surgical view. Movie S9B corresponds to this panel

a valve with two orifices.<sup>39</sup> In the case of myxomatous mitral valve regurgitation, especially in the presence of a prolapsing leaflet, this procedure effectively restores valvular competence.<sup>40</sup> The relative

simplicity and reproducibility of Alfieri's edge-to-edge technique have made this procedure a reliable tool for restoring prolapsed anterior and posterior leaflets.<sup>41</sup>



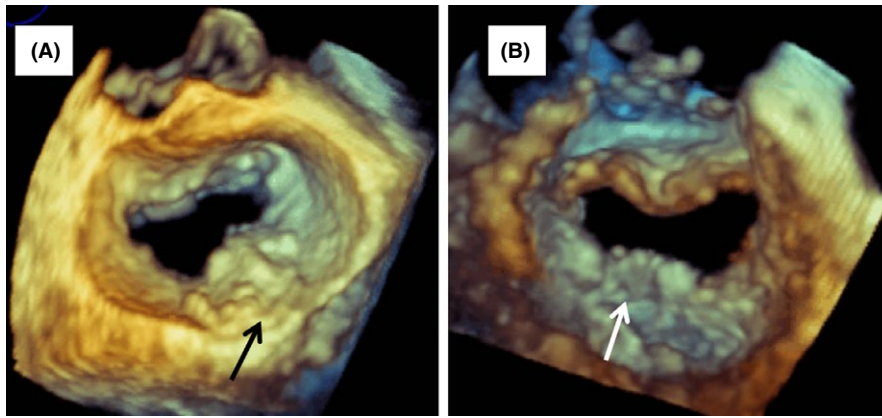


**FIGURE 13** Ringless mitral annuloplasty. A and B. 3DTEE appearance of ringless annuloplasty and quadrangular resection of the posterior leaflet (arrow) from the left atrial (A) and left ventricular perspective (B) in the standard surgical view. Movie S10 corresponds to this panel

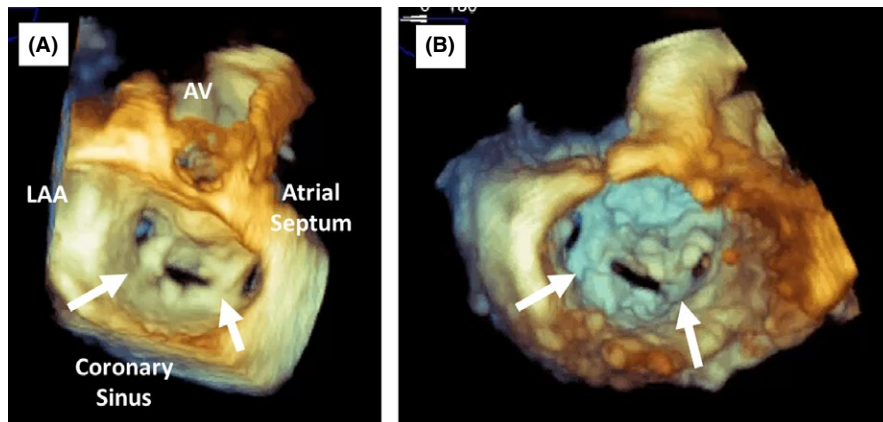


**FIGURE 14** Surgical edge-to-edge technique (Alfieri Stitch). A and B. 3DTEE appearance of a mitral valve status post the edge-to-edge technique from the left atrial (A) and left ventricular (B) perspective in the standard surgical view. Arrows point to two Alfieri stitches. Movie S11 corresponds to these figure panels

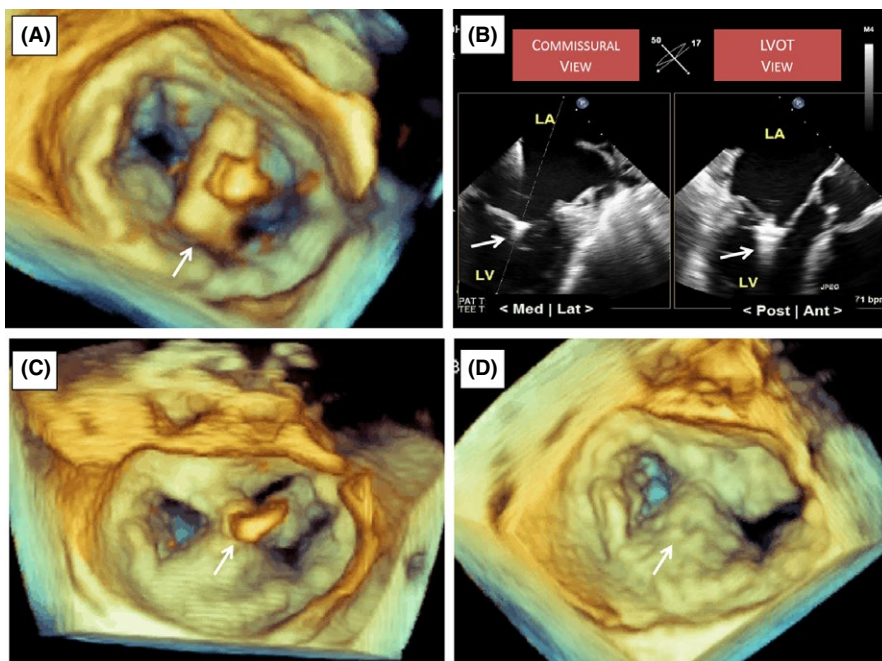


**FIGURE 15** 3DTEE guidance of percutaneous edge-to-edge technique (mitral clipping). Stepwise guidance of mitral clipping on 3DTEE from clip alignment in the left atrium above the flail P2 scallop (A), advancement of the clip into the left ventricle (B), initial grasping of the two mitral leaflets at the A2/P2 coaptation line (C), and final clip release (D). Movie S12 corresponds to these figure panels

Mitral annuloplasty ring is depicted in Figure 11, mitral annuloplasty band in Figure 12, and ringless mitral annuloplasty in Figure 13. A mitral repair using the surgical edge-to-edge technique is depicted in Figure 14. Each figure contains corresponding movies.

## 9 | MITRACLIP

The MitraClip (Abbott Vascular, Santa Clara, CA, USA) is a percutaneous version of the Alfieri edge-to-edge technique which has recently



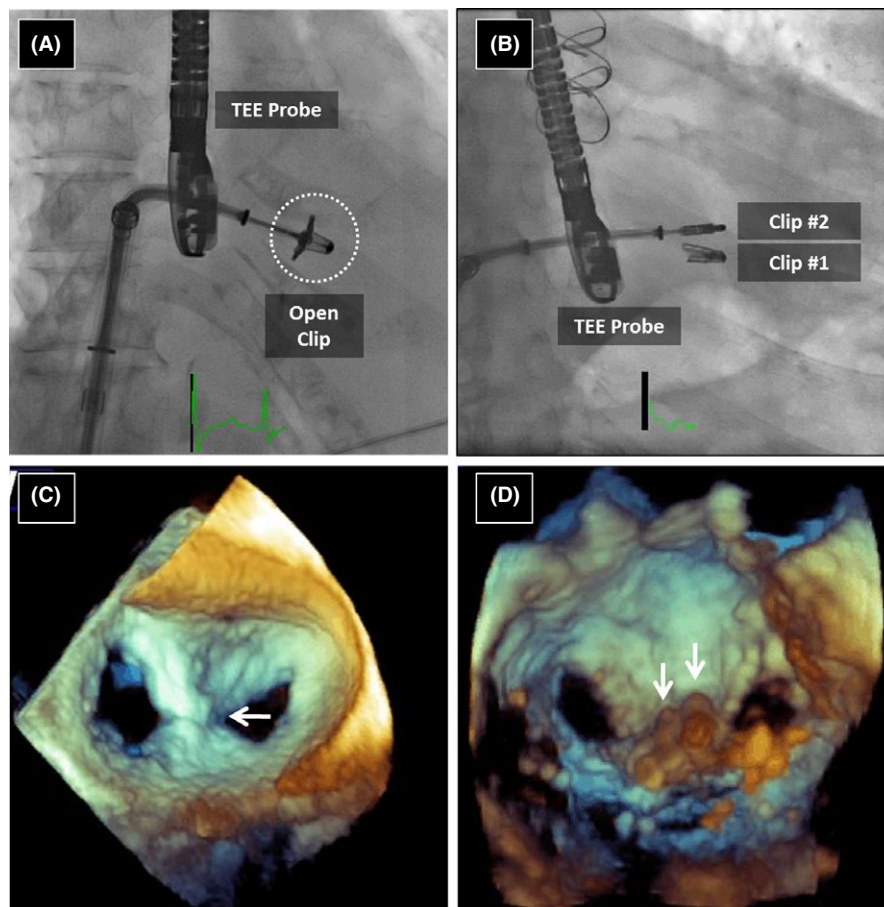


**FIGURE 16** Percutaneous edge-to-edge technique (mitral clipping). A and B. Radiographic appearance of MitraClip during fluoroscopy. A. demonstrates open MitraClip prior to clip deployment. B. demonstrates two MitraClips; one fully deployed (Clip #1) and the other in the process of deployment (Clip #2). C and D. 3DTEE appearance of mitral valve status post placement of MitraClips (arrows) from the left atrial (C) and left ventricular (D) perspective in the standard surgical view. AML = anterior mitral leaflet; AV = aortic valve; PML = posterior mitral leaflet. Movie S13 corresponds to Panel C and Panel D

been approved in the United States for the treatment of moderate-to-severe or severe symptomatic, degenerative mitral valve regurgitation in patients with high surgical risk. The MitraClip is “comprised of arms joined together by a hinge and grippers.”<sup>42</sup> Real time 3DTEE is essential for guidance of this procedure, as it allows the physician to grasp the mitral leaflets and approximate with a polyester-covered clip, yielding the edge-to-edge coaptation analogous to that achieved surgically.<sup>42</sup> Furthermore, an added benefit of the use of real time 3DTEE is the ability to assess the clip immediately after insertion as it experiences the near normal forces of diastolic flow in the beating heart.<sup>43</sup>

Most recently, the prospective, multicenter Endovascular Valve Edge-to-Edge Repair Study (EVEREST) II sought to analyze the role of the MitraClip in the treatment of mitral regurgitation as compared to surgical intervention.<sup>44</sup> The study found that at the four- and five-year follow-up time, patients with MitraClip repair “more commonly required surgery for residual MR during the first year after treatment, but between 1- and 5-year follow-up there were comparably low rates of surgery for MV dysfunction with either percutaneous or surgical therapy.”<sup>45</sup> The current results of the EVEREST II trial reveal that although surgery is currently superior to the MitraClip in reducing mitral regurgitation, the MitraClip does prove to be beneficial in reducing symptomatology and favorable reverse remodeling of the ventricle after five years.<sup>45</sup> Additional follow-up will be needed to determine if there are long-term effects on mortality for the two cohorts.

A percutaneous edge-to-edge repair (MitraClip) is depicted in Figure 15 and Figure 16 and corresponding movies.

## 10 | CONCLUSION

This paper reviews the appearance of mitral valve prostheses and mitral valve repair using 3DTEE and provides a historical context for these advancements. As comprehensive collections of 3DTEE images of surgical and percutaneous interventions are not commonly found in the current literature, we feel that clinicians can benefit from this manuscript and use it as a guide to these interventions.

## ACKNOWLEDGMENTS

We thank Drs. Itzhak Kronzon and Gila Perk from the Department of Cardiovascular Medicine at Lenox Hill Hospital, New York, NY for their contribution.

## REFERENCES

1. Williams JB, inventor, assignee. Improved Bottle Stopper. US patent 19,323. 1858 Feb 9.
2. Lang RM, Tsang W, Weinert L, Mor-Avi V, Chandra S. Valvular heart disease. The value of 3-dimensional echocardiography. *J Am Coll Cardiol*. 2011;58:1933–1944.

3. Benenstien R, Saric M. Mitral valve prolapse: role of 3D echocardiography in diagnosis. *Curr Opin Cardiol*. 2012;27:465–476.
4. Kurklinsky A, Mankad S. Three-dimensional echocardiography in valvular heart disease. *Cardiol Rev*. 2012;20:66–71.
5. Wernly JA, Crawford MH. Choosing a prosthetic heart valve. *Cardiol Clin*. 1991;9:329–338.
6. Gott VL, Alejo DE, Cameron DE. Mechanical heart valves: 50 years of evolution. *Ann Thorac Surg*. 2003;76:S2230–S2239.
7. Zilla P, Brink J, Human P, Bezuidenhout D. Prosthetic heart valves: catering for the few. *Biomaterials*. 2008;29:385–406.
8. van den Brink RB, Visser CA, Basart DC, Düren DR, de Jong AP, Dunning AJ. Comparison of transthoracic and transesophageal color Doppler flow imaging in patients with mechanical prostheses in the mitral valve position. *Am J Cardiol*. 1989;63:1471–1474.
9. Fuster V, Pumphrey CW, McGoon MD, Chesebro JH, Pluth JR, McGoon DC. Systemic thromboembolism in mitral and aortic Starr-Edwards prostheses: a 10–19 year follow-up. *Circulation*. 1982;66:157–161.
10. Flachskampf FA, O'Shea JP, Griffin BP, Guerrero L, Weyman AE, Thomas JD. Patterns of normal transvalvular regurgitation in mechanical valve prostheses. *J Am Coll Cardiol*. 1991;18:1493–1498.
11. DeWall RA, Qasim N, Carr L. Evolution of mechanical heart valves. *Ann Thorac Surg*. 2000;69:1612–1621.
12. Vongpatanasin W, Hillis LD, Lange RA. Prosthetic heart valves. *N Engl J Med*. 1996;335:407–416.
13. Björk VO. The pyrolytic carbon occluder for the Björk-Shiley tilting disc valve prosthesis. *Scand J Thorac Cardiovasc Surg*. 1972;6:109–113.
14. Taams MA, Gussenhoven EJ, Cahalan MK, et al. Transesophageal Doppler color flow imaging in the detection of native and Björk-Shiley mitral valve regurgitation. *J Am Coll Cardiol*. 1989;13:95–99.
15. Edwards MS, Russell GB, Edwards AF, Hammon JW Jr, Cordell AR, Kon ND. Results of valve replacement with Omniscience mechanical prostheses. *Ann Thorac Surg*. 2002;74:665–670.
16. Butany J, Ahluwalia MS, Munroe C, et al. Mechanical heart valve prostheses: identification and evaluation. *Cardiovasc Pathol*. 2003;12:1–22.
17. Yoganathan AP, He Z, Casey Jones S. Fluid mechanics of heart valves. *Annu Rev Biomed Eng*. 2004;6:331–362.
18. Butchart EG, Li HH, Payne N, Buchan K, Grunkemeier GL. Twenty years' experience with the Medtronic Hall valve. *J Thorac Cardiovasc Surg*. 2001;121:1090–1100.
19. Dellsperger KC, Wieting DW, Baehr DA, Bard RJ, Brugger JP, Harrison EC. Regurgitation of prosthetic heart valves: dependence on heart rate and cardiac output. *Am J Cardiol*. 1983;51:321–328.
20. Czer L, Matloff J, Chaux A, Derobertis M, Yoganathan A, Gray RJ. A 6-year experience with the St. Jude Medical valve: hemodynamic performance, surgical results, biocompatibility, and follow-up. *J Am Coll Cardiol*. 1985;6:904–912.
21. Emery RW, Krogh CC, Arom KV, et al. The St. Jude Medical cardiac valve prosthesis: a 25-year experience with single valve replacement. *Ann Thorac Surg*. 2005;79:776–783.
22. Otto CM, Bonow RO. *Otto & Bonow Valvular Heart Disease: A Companion to Braunwald's Heart Disease*. 3rd ed. Philadelphia: Elsevier Health Sciences; 2009: p. 384.
23. Misawa Y, Taguchi M, Aizawa K, et al. Twenty-two year experience with the omniscience prosthetic heart valve. *ASAIO J*. 2004;50:606–610.
24. Bryan AJ, Rogers CA, Bayliss K, Wild J, Angelini GD. Prospective randomized comparison of CarboMedics and St. Jude Medical bileaflet mechanical heart valve prostheses: ten-year follow-up. *J Thorac Cardiovasc Surg*. 2007;133:614–622.
25. Johnston RT, Weerasena NA, Butterfield M, Fisher J, Spyt TJ. CarboMedics and St. Jude Medical bileaflet valves: an in vitro and in vivo comparison. *Eur J Cardiothorac Surg*. 1992;6:267–271.
26. Harrison EC, Rashtian MY, Allen DT, Yoganathan AP, Rahimtoola SH. An emergency physician's guide to prosthetic heart valves: identification and hemodynamic function. *Ann Emerg Med*. 1988;17:194–200.
27. Aslam AK, Aslam AF, Vasavada BC, Khan IA. Prosthetic heart valves: types and echocardiographic evaluation. *Int J Cardiol*. 2007;122:99–110.
28. Jamieson WR, Munro AI, Miyagishima RT, Allen P, Burr LH, Tyers GF. Carpentier-Edwards standard porcine bioprosthesis: clinical performance to seventeen years. *Ann Thorac Surg*. 1995;60:999–1006. discussion 1007.
29. Carpentier A, Lemaigre G, Robert L, Carpentier S, Dubost C. Biological factors affecting long-term results of valvular heterografts. *J Thorac Cardiovasc Surg*. 1969;58:467–483.
30. Gao G, Wu Y, Grunkemeier GL, Furnary AP, Starr A. Durability of pericardial versus porcine aortic valves. *J Am Coll Cardiol*. 2004;44:384–388.
31. Goetze S, Brechtken J, Agler DA, Thomas JD, Sabik JF 3rd, Jaber WA. In vivo short-term Doppler hemodynamic profiles of 189 Carpentier-Edwards Perimount pericardial bioprosthetic valves in the mitral position. *J Am Soc Echocardiogr*. 2004;17:981–987.
32. Feneck R, Kneeshaw J. *Core Topics in Transesophageal Echocardiography*. New York: Cambridge University Press; 2010:312.
33. Pibarot P, Dumesnil JG. Doppler echocardiographic evaluation of prosthetic valve function. *Heart*. 2012;98:69–78. <https://doi.org/10.1136/heartjnl-2011-300351>.
34. Lázaro C, Hinojar R, Zamorano JL. Cardiac imaging in prosthetic paravalvular leaks. *Cardiovasc Diagn Ther*. 2014;4:307–313.
35. Klinger C, et al. Review of surgical prosthetic paravalvular leaks: diagnosis and catheter-based closure. *Eur Heart J*. 2013;34:638–649.
36. Seiffert M, Conradi L, Baldus S, et al. Transcatheter Mitral Valve-in-Valve Implantation in Patients With Degenerated Bioprostheses. *JACC Cardiovasc Interv*. 2012;5:341–349.
37. Carpentier A, Relland J, Deloche A, et al. Conservative management of the prolapsed mitral valve. *Ann Thorac Surg*. 1978;26:294–302.
38. Rausch MK, Bothe W, Kvitting JP, Swanson JC, Miller DC, Kuhl E. Mitral valve annuloplasty: a quantitative clinical and mechanical comparison of different annuloplasty devices. *Ann Biomed Eng*. 2012;40:750–761. Epub 2011 Oct 25.
39. Wong RH, Lee AP, Ng CS, Wan IY, Wan S, Underwood MJ. Mitral valve repair: past, present, and future. *Asian Cardiovasc Thorac Ann*. 2010;18:586–595.
40. Maisano F, Skantharaja R, Denti P, Giacomini A, Alfieri O. Mitral annuloplasty. *Multimed Man Cardiothorac Surg*. 2009;2009:mmcts.2008.003640.
41. Barlow CW, Ali ZA, Lim E, Barlow JB, Wells FC. Modified technique for mitral repair without ring annuloplasty. *Ann Thorac Surg*. 2003;75:298–300.
42. Maisano F, Caldarola A, Blasio A, De Bonis M, La Canna G, Alfieri O. Midterm results of edge-to-edge mitral valve repair without annuloplasty. *J Thorac Cardiovasc Surg*. 2003;126:1987–1997.
43. Fedak PW, McCarthy PM, Bonow RO. Evolving concepts and technologies in mitral valve repair. *Circulation*. 2008;117:963–974.
44. David TE, Armstrong S, Ivanov J. Chordal replacement with polytetrafluoroethylene sutures for mitral valve repair: A 25-year experience. *J Thorac Cardiovasc Surg*. 2013;145:1563–1569.
45. Kotoulas C, Omorphos S, Sarraf A, Patris K, Hasan R. Mitral valve repair: beyond the French correction. *Hellenic J Cardiol*. 2008;49:329–334.
46. Dang NC, Aboodi MS, Sakaguchi T, et al. Surgical revision after percutaneous mitral valve repair with a clip: initial multicenter experience. *Ann Thorac Surg*. 2005;80:2338–2342.
47. Zoghbi WA, Enriquez-Sarano M, Foster E, et al. American Society of Echocardiography: Recommendations for evaluation of the severity of native valvular regurgitation with two-dimensional and Doppler echocardiography. *J Am Soc Echocardiogr*. 2003;16:777–802.
48. Mauri L, et al. 4-Year results of a randomized controlled trial of percutaneous repair versus surgery for mitral regurgitation. *J Am Coll Cardiol*. 2013;62:317–328.

49. Feldman T. Randomized comparison of percutaneous repair and surgery for mitral regurgitation 5-year results of EVEREST II. *J Am Coll Cardiol*. 2015;66:2844–2854.

## SUPPORTING INFORMATION

Additional Supporting Information may be found online in the supporting information tab for this article.

**Movie S1A.** Starr–Edwards mechanical prosthesis in the mitral position visualized on fluoroscopy.

**Movie S1B.** 3DTEE of a mitral Starr–Edwards valve. In the first portion of the video, the valve is seen on a 3D zoom imaging from the left atrial perspective. In the second portion, the valve is seen from LV perspective, and in the third portion, the valve is seen in its long axis on color Doppler imaging.

**Movie S2A.** Bjork–Shiley mechanical prosthesis in the mitral position visualized on fluoroscopy.

**Movie S2B.** Bjork–Shiley mechanical prosthesis in the mitral position is seen on a 3D zoom imaging from the left atrial perspective.

**Movie S3A.** 3DTEE of a Medtronic–Hall mechanical prosthesis in the mitral position visualized first from the left atrial followed by the left ventricular perspective.

**Movie S3B.** Aortic and mitral Medtronic–Hall mechanical prostheses visualized by fluoroscopy.

**Movie S4A.** St Jude mechanical prosthesis in the mitral position visualized on fluoroscopy.

**Movie S4B.** 3DTEE of a St Jude mechanical prosthesis in the mitral position visualized first from the left atrial perspective.

**Movie S5A.** Omniscience mechanical prosthesis in the mitral position visualized on fluoroscopy.

**Movie S5B.** 3DTEE of an Omniscience mechanical prosthesis in the mitral position visualized first from the left atrial perspective.

**Movie S6A.** A mitral bioprosthesis visualized on fluoroscopy.

**Movie S6B.** 3DTEE of a mitral bioprosthesis visualized first from the left atrial followed by the left ventricular perspective.

**Movie S7.** Mitral valve-in-valve implantation

**Movie S8A.** A mitral annuloplasty ring visualized on fluoroscopy.

**Movie S8B.** 3DTEE of a mitral annuloplasty ring visualized first from the left atrial perspective.

**Movie S9A.** A mitral annuloplasty band visualized on fluoroscopy.

**Movie S9B.** 3DTEE of a mitral annuloplasty band visualized first from the left atrial followed by the left ventricular perspective.

**Movie S10.** 3DTEE of a ringless mitral annuloplasty visualized first from the left atrial followed by the left ventricular perspective.

**Movie S11.** 3DTEE of an Alfieri stitch (edge-to-edge repair) visualized first from the left atrial followed by the left ventricular perspective.

**Movie S12.** 3DTEE guidance of mitral clipping

**Movie S13.** 3DTEE of percutaneous mitral clipping visualized first from the left atrial followed by the left ventricular perspective.

**How to cite this article:** Jafar N, Moses MJ, Benenstein RJ, et al. 3D transesophageal echocardiography and radiography of mitral valve prostheses and repairs. *Echocardiography*. 2017;34:1687–1701. <https://doi.org/10.1111/echo.13656>

Copyright of Echocardiography is the property of Wiley-Blackwell and its content may not be copied or emailed to multiple sites or posted to a listserv without the copyright holder's express written permission. However, users may print, download, or email articles for individual use.